広島大学学術情報リポジトリ
Hiroshima University Institutional Repository

Title	Transformation of LEV-type zeolite into less dense CHA-type zeolite
Author(s)	Goto, Ikuhiro; Itakura, Masaya; Shibata, Syohei; Honda, Koutaro; Ide, Yusuke; Sadakane, Masahiro; Sano, Tsuneji
Citation	Microporous and Mesoporous Materials , 158 : 117 - 122
Issue Date	2012
DOI	10.1016/j.micromeso.2012.03.032
Self DOI	
URL	https://ir.lib.hiroshima-u.ac.jp/00034806
Right	(c) 2012 Elsevier Inc. All rights reserved.
Relation	

Transformation of LEV-type zeolite into less dense CHA-type zeolite

Ikuhiro Goto, Masaya Itakura, Syohei Shibata, Koutaro Honda, Yusuke Ide, Masahiro

Sadakane, Tsuneji Sano*

Department of Applied Chemistry, Graduate School of Engineering, Hiroshima

University, Higashi-Hiroshima 739-8527, Japan

Phone: +81-82-424-7607

Fax: +81-82-424-5494

E-mail: tsano@hiroshima-u.ac.jp

Abstract

Hydrothermal conversion of LEV-type zeolite into CHA-type zeolite occurred in the

absence of both an organic structure-directing agent and a seed crystal. The LEV-CHA

transformation proceeds from a more dense zeolite (LEV) to a less dense one (CHA).

When amorphous aluminosilicate hydrogels were used as starting materials, the

CHA-type zeolite was not obtained under the present hydrothermal synthesis

conditions. From the fact that the LEV-CHA transformation proceeded at lower alkalinity conditions, it was suggested that locally ordered aluminosilicate species (nanoparts) produced by decomposition/dissolution of the starting LEV-type zeolite contribute to the transformation process. On the other hand, at higher alkalinity than that used for the CHA-type zeolite synthesis, LEV-LTA transformation occurred effectively and selectively. These results suggest that there is a large difference in the structures of nanoparts generated by decomposition/dissolution of the starting zeolite in the LEV-CHA and LEV-LTA transformations.

Keywords: Hydrothermal conversion, Interzeolite conversion, LEV-type zeolite, CHA-type zeolite, Less dense zeolite

1. Introduction

In general, medium/large pore size and high-silica zeolites are synthesized by hydrothermal treatment of amorphous aluminosilicate hydrogel as a starting material in the presence of organic structure-directing agents (OSDAs). The use of OSDAs is, however, undesirable from a practical point of view, because of their high cost as well

as their large environmental impact. As a consequence of these drawbacks, the synthesis of zeolites from seed crystals without the use of OSDAs has attracted considerable attention, and several research groups have already succeeded in the OSDA-free synthesis of ECR-1 [1], ZSM-34 [2], *BEA [3−5], **ZSM-5 [6],** RTH [7], ZSM-12 [8], and EMT [9] zeolites.

In the synthesis of most zeolites, an amorphous phase is **<u>converted into a given type of zeolite by the solution-mediated transformation process [10]</u>**. Because zeolites are metastable, however, a sequence from the amorphous phase → a less stable zeolite → the most stable zeolite is often observed. **<u>Although the transformation to the most stable zeolite is thermodynamically driven, final phase selection is controlled by the interplay of nucleation, growth and phase transformation kinetics.</u>** Theoretical calculations and calorimetric measurements have suggested that the stability of zeolites decreases as their porosity increases, that is, as the zeolite framework density decreases [11,12]. On this basis, several research groups have pointed out the high potential of an alternative method for zeolite formation, i.e., the hydrothermal conversion of one zeolite type into another (interzeolite conversion) [13−15].

Recently, our group has also investigated the potential of interzeolite conversion and has succeeded in synthesizing several types of zeolites, such as *BEA- [16], RUT- [17],

CHA- [18], LEV- [19], MTN- [20], and OFF-type zeolites [21] using FAU-type zeolite as the starting material in the presence of various OSDAs. **Among the zeolites synthesized, LEV- and CHA-type zeolites with eight-membered ring pores (4.8 × 3.6 Å) have attracted considerable interest because they show shape-specific selectivity for the conversion of methanol or ethanol into light olefins such as ethylene and propylene.** The use of FAU-type zeolite as a starting material for the preparation of other zeolites, in the presence of choline hydroxide as an OSDA for LEV-type zeolite and benzyltrimethylammonium hydroxide as an OSDA for CHA-type zeolite, results in a crystallization rate that is superior to that achieved in the conventional synthesis using amorphous aluminosilicate gel as the starting material. This enhanced crystallization rate arises because the decomposition/dissolution of the starting zeolite generates locally ordered aluminosilicate species (nanoparts) that assemble and evolve into another type of zeolite [22].

In addition to the successful interzeolite conversions achieved using OSDAs, we very recently succeeded in OSDA-free FAU-*BEA [23] and FAU-LEV [24] transformations using corresponding noncalcined seed crystals. Although the seed crystals employed contained OSDA cations in the zeolitic pores, no additional OSDAs were added into the starting gels. **In contrast, when the calcined seed crystals were employed, no**

crystalline products were obtained. Namely, the XRD peaks due to seed crystals as well as the starting FAU-type zeolite disappeared completely even after only 30 min of hydrothermal treatment [24]. The OSDA cations in the zeolitic pores stabilized the seed crystals, and, consequently, the crystal surfaces of the seed crystals contributed to the crystal growth of the *BEA- and LEV-type zeolites. An investigation of the framework structures of these FAU-, *BEA-, and LEV-type zeolites revealed that there is a similar building unit in their frameworks, the linear connection of four-membered rings.

Taking into account the fact that LEV- and CHA-type zeolites have similar composite building units, because the two zeolites both belong to the chabazite group, the above results strongly suggest that it is possible to synthesize CHA-type (LEV-type) zeolite without the use of both OSDAs and seed crystals, if the starting LEV-type (CHA-type) zeolite is decomposed/dissolved into locally ordered aluminosilicate species (nanoparts) whose chemical structures are suitable for the crystallization of CHA-type (LEV-type) zeolite. This process would just involve reassembly of the nanoparts. Therefore, we applied the interzeolite conversion method to the OSDA-free, seed-crystal–free synthesis of CHA-type zeolite with a framework density (FD) of 15.1 T/1000 Å^3 from LEV-type zeolite with a FD of 15.9 T/1000 Å^3. That is, we transformed LEV-type

zeolite into less dense CHA-type zeolite. **Taking into consideration that thermodynamic stability of zeolite decreases with decreasing framework density, transformation of thermodynamically stable LEV-type zeolite into thermodynamically less stable CHA-type zeolite is not possible from the thermodynamic standpoint. However, if CHA phase is a metastable state during transformation towards the most stable state, it is possible to observe crystallization of CHA-type zeolite in a kinetically controlled process.**

The possibility of transforming zeolite into less dense zeolites, for example, transforming ANA-type zeolite (FD = 19.2 T/1000 $\AA^3$) into KFI-type zeolite (FD = 15 T/1000 $\AA^3$), has already **been** reported by Barrer et al. [25]. However, this report did not provide information concerning the details of the transformation behavior. Very recently, Zicovich-Wilson et al. reported the transformation of TON-type zeolite (FD = 18.1 T/1000 $\AA^3$) into less dense ITW-type zeolite (FD = 17.7 T/1000 $\AA^3$), although this transformation required both 1,3,4-trimethylimidazolium and fluoride ions [26]. Tian et al. also reported the phase transformation synthesis of SAPO-34 from SAPO-5 using dimethylamine [27]. To our knowledge, this is the first report on the transformation of LEV-type zeolite into less dense CHA-type zeolite without the use of both seed crystals and OSDAs.

2. Experimental

2.1. Synthesis of starting LEV

To produce the starting material, LEV-type zeolites with various Si/Al ratios were synthesized from FAU-type zeolites with different Si/Al ratios using choline hydroxide as a SDA according to the procedure described in our previous report [19]. The obtained LEV-type zeolites were calcined at 450 °C for 48 h to remove choline cations from the zeolitic pores. The prepared LEV-type zeolites had a well-defined LEV structure, as demonstrated by the XRD pattern (Figure 1(a)). No diffraction peaks other than those of the LEV phase were observed. As can be seen in Figure 2(a), SEM observations revealed a round morphology of the LEV-type zeolite (Sample no. 1). The BET surface area and micropore volume were calculated to be 560 m^2 g^{-1} and 0.26 cm^3 g^{-1}, respectively.

2.2. Hydrothermal conversion of LEV into CHA

Hydrothermal conversion of LEV-type zeolite into CHA-type zeolite was carried out by adding the prepared LEV-type zeolite to an aqueous solution of MOH (M: alkaline metal). The mixtures **with chemical compositions of Si/Al = 6 – 22, $NaOH/SiO_2$ = 3,**

7

and H₂O/SiO₂ = 80 were placed into a 30-cm³ Teflon-lined stainless steel autoclave. Hydrothermal conversion was conducted under static conditions at 90–200 °C for 1.5–24 h in a convection oven. The solid product was collected by centrifugation and washed thoroughly with deionized water until the pH was near neutral. Then, it was dried overnight at 70 °C and then calcined at 550 °C for 10 h. The details of the hydrothermal conversion conditions are listed in Table 1. **For comparison, starting gels from the following Si and Al sources were also prepared: Cab-O-Sil M-5 (SiO₂ = 99.8 wt%, Fluka) and NaAlO₂ (Al₂O₃ = 70 wt%, Kishida Chemical Inc. Japan). Ca²⁺-ion-exchanged form was prepared by multitreatment(3 times) of the calcined form(Na⁺ form) with 1 M CaCl₂ (Kanto Chemical Co Inc., Japan) aqueous solution at 60 °C for 2 h, followed by washing to remove the chloride ions.**

2.3. Characterization

X-ray diffraction (XRD) patterns of the solid products were collected using a powder X-ray diffractometer (Rigaku, Mini Flex) with graphite-monochromatized Cu Kα radiation at 30 kV and 15 mA. The bulk Si/Al ratios were determined using inductively coupled plasma optical emission spectroscopy (ICP, Seiko SPS7000). The crystal morphology was observed using scanning electron microscopy (SEM, Hitachi S-4800).

The ^{27}Al magic angle spinning (MAS) NMR and ^{29}Si MAS NMR spectra were recorded at 104.2 MHz and 79.5 MHz, respectively, on a Varian 600PS solid NMR spectrometer, using a 3.2-mm-diameter zirconia rotor for ^{27}Al MAS NMR and a 6-mm-diameter zirconia rotor for ^{29}Si MAS NMR. The rotor was spun at 6 kHz for ^{29}Si MAS NMR and at 15 kHz for ^{27}Al MAS NMR. The spectra were acquired using 2.3 μs pulses, a 1 s recycle delay, and 1000 scans for ^{27}Al MAS NMR, and 5 μs pulses, a 100 s recycle delay, and 1000 scans for ^{29}Si MAS NMR. Al(NO$_3$)$_3$·9H$_2$O and Si(CH$_3$)$_4$ were used as chemical shift references for ^{27}Al and ^{29}Si MAS NMR, respectively. Prior to the ^{27}Al MAS NMR measurements, the samples were moisture-equilibrated over a saturated solution of NH$_4$Cl for 24 h. Nitrogen adsorption isotherms at −196 °C were obtained using a conventional volumetric apparatus (Bel Japan, BELSORP-mini). Prior to the adsorption measurements, the samples (ca. 0.1 g) were evacuated at 400 °C for 10 h.

3. Results and Discussion

3.1. Transformation of LEV into CHA

First, we investigated the transformation behavior of LEV-type zeolite with a Si/Al ratio of 9 (Sample no.1). Several preliminary experiments allowed the NaOH/SiO$_2$ and H$_2$O/SiO$_2$ ratios in the starting materials to be fixed at 3.0 and 80, respectively. Detailed

synthesis conditions and characteristics of the products obtained are listed in Table 1. Figure 1 shows the XRD patterns of the products obtained by varying the hydrothermal treatment time. It is clear that the starting LEV-type zeolite decomposed into an amorphous phase, and then the pure CHA-type zeolite crystallized after 1.5 h of hydrothermal treatment. As the treatment time increased, the peaks corresponding to the CHA phase decreased, **and the peaks corresponding to GIS and ANA phases together with a small amount of FAU phase were observed after 8 h of hydrothermal treatment. Finally, the pure ANA-type zeolite was obtained after 24 h. Although GIS-, ANA- and FAU-type zeolites were formed from amorphous aluminosilicate hydrogesl prepared using Cab-O-Sil M-5 and NaAlO$_2$, the formation of CHA-type zeolite was not observed (see supplementary information Figure 1S).** In other words, a sequence from starting LEV → an amorphous phase → CHA → ANA was observed. The diffraction pattern of the obtained CHA-type zeolite was typical of CHA structure and contained no impurity peaks from unconverted starting LEV-type zeolite or cocrystallized phases. This indicates that the metastable CHA-type zeolite crystallizes in a kinetically controlled process and that the transformation to the most stable ANA-type zeolite is thermodynamically driven. To the best of our knowledge, this is the first report on the transformation of LEV-type zeolite

into less dense CHA-type zeolite without the use of both seed crystals and OSDAs. The yield of CHA-type zeolite was 19% based on the weight of the **starting** LEV-type zeolite. Figures 2(b) and 2(c) show SEM images of the obtained CHA-type zeolites. The crystal morphology was cubic, and the crystals were 200–400 nm in size, which is smaller than the crystal size of the starting LEV-type zeolite, as shown in Figure 2(a).

The chemical state of the aluminum in the obtained CHA-type zeolite was investigated using ^{27}Al MAS NMR spectroscopy. As shown in Figure 3(a), the ^{27}Al MAS NMR spectrum of the CHA-type zeolite showed only the peak at approximately 56 ppm, corresponding to tetrahedrally-coordinated framework aluminum species. No peak corresponding to octahedrally-coordinated aluminum species (which is indicative of extra-framework aluminum species) was observed at around 0 ppm. **Although there is a possibility of the formation of invisible aluminum species [28, 29],** this implies that all of the aluminum species existed within the zeolite framework in the CHA-type zeolite obtained via the hydrothermal conversion of LEV-type zeolite in the absence of any OSDAs and seed crystals.

The ^{29}Si MAS NMR spectrum of the obtained CHA-type zeolite, presented in Figure 3(b), showed five peaks at –108, –103, -98, –92, and –88 ppm. These peaks can be assigned to Si(0Al), Si(1Al), Si(2Al), Si(3Al), and Si(4Al) species, respectively [30].

The existence of the Si(4Al) species indicates that the obtained CHA-type zeolite has a high aluminum content. The bulk Si/Al ratio measured using ICP was actually 2.8, which is considerably lower than that of the starting LEV-type zeolite (Si/Al = 9). This is probably a result of the highly alkaline conversion conditions, which caused an increase in the silicon concentration in the liquid phase.

As can be seen in Figure 4(a), the amount of nitrogen adsorbed on the Na^+-ion-exchanged CHA-type zeolite was small. This is probably due to the pore blocking at particular locations by Na^+-cations, which behave as charge compensators, or the presence of amorphous alumina and silica. Taking into account that there was no peak corresponding to octahedrally-coordinated aluminum species at around 0 ppm (Figure 3(a)), the existence of amorphous material in the zeolite pores seems to be unlikely. On the other hand, the nitrogen adsorption isotherm of the Ca^{2+}-ion-exchanged CHA-type zeolite can be classified as type I based on the IUPAC classification (Figure 4(b)), and the BET surface area and micropore volume were calculated to be 260 m^2 g^{-1} and 0.12 cm^3 g^{-1}, respectively. These values are slightly smaller than those of the CHA-type zeolite synthesized from FAU-type zeolite and KOH according to the method described in *"Verified Syntheses of Zeolitic Materials"* published by the International Zeolite Association, 340 m^2 g^{-1} and 0.17 cm^3 g^{-1} [31]. **Although we could not explain**

12

the exact reason for lower BET surface area and micropore volume of Ca^{2+}-ion-exchanged CHA-type zeolite at the present time, it is probably due to the lower crystallinity.

Previous studies undertaken by this group indicated that interzeolite conversion was strongly dependent on the Si/Al ratio of the starting zeolite [16−21]. Therefore, the influence of the Si/Al ratio of the starting LEV-type zeolite on the CHA-type zeolite synthesis was investigated herein using LEV-type zeolites with various Si/Al ratios (Si/Al = 6−22). The results presented in Table 1 indicate that LEV-type zeolites with Si/Al ratios in the range of 9−12 could be converted into pure CHA-type zeolites by employing a synthesis time of 1.5 h (Sample nos. 1, 3, 5, and 8). The yield of **CHA**-type zeolite was ca. 20% regardless of the Si/Al ratio of the starting LEV-type zeolite. When LEV-type zeolite with a Si/Al ratio of 22 was used, no product was obtained. **Namely, LEV-type zeolite was completely dissolved without subsequent transformation. It seems to be due to the enhancement of dissolution rate of LEV-type zeolite with a high Si/Al ratio. It is well recognized that the rate of dissolution of aluminosilicate materials in alkaline solutions increases with increasing Si/Al ratio [32,33]. On the other hand, in the case of LEV-type zeolite with a Si/Al ratio of 6, the starting zeolite hardly decomposed due to the lower dissolution rate, indicating that a**

longer crystallization time is needed. At the present time, we could not explain exactly why the yield of CHA-type zeolite is independent on the Si/Al ratio of starting LEV-type zeolite, probably due to the interplay of decomposition/dissolution, nucleation, growth, and phase transformation kinetics.

We then studied the influence of the synthesis temperature. When the hydrothermal conversion of LEV-type zeolite was carried out at 125−170 °C for 1.5 h, the LEV-type zeolite was transformed into CHA-type zeolite. At 200 °C, pure ANA-type zeolite was obtained, suggesting that CHA-type zeolite transformed into the most stable zeolite. At 90 °C, pure CHA zeolite was obtained when the synthesis time was prolonged to 12 h. The morphology and crystal size of the **CHA**-type zeolite crystals obtained at 90 °C were similar to those obtained at 125 °C.

Finally, the influences of various types of alkaline metal cations were investigated. As shown in Table 1, when LiOH, KOH, and RbOH were employed instead of NaOH as an alkali source, the transformation of LEV-type zeolite did not occur (Sample nos. 9−11). Although we do not have enough data to explain this difference, we speculate as follows. **Assuming that locally ordered aluminosilicates generated from the starting LEV-type zeolte are precursor species for nucleation and crystal growth of CHA-type zeolite and taking into consideration that the basicity of alkaline metal**

increases in the sequence: LiOH < NaOH< KOH < RbOH, one can expect that the rate of LEV-CHA transformation would increase in the same sequence. However, formation of amorphous phase without subsequent formation of CHA-type zeolite (at least for 1.5 h of hydrothermal treatment) when LiOH, KOH and RbOH are used as mineralizing agents indicates that the structured precursor species are formed by the structure-forming action of Na$^+$ ion to the silicate and aluminate species obtained by decomposition/dissolution of LEV-type zeolite; such precursor species are not formed in the presence of structure-breaking K$^+$ and Rb$^+$ ions [34]. Although, Li$^+$ ion is formally the structure-forming cation, it seems that its lower basicity prevail the structure-forming ability, i.e., it can be expected that the process of transformation in LiOH is considerably slower than that in NaOH and, thus 1.5 h of hydrothermal treatment is too short time interval for the formation of measurable amounts of CHA-type zeolite. However, we could not rule out the following possibility, another type of zeolite different from CHA-type zeolite is the most stable in Li$^+$ ion environment.

3.2. Effects of NaOH/SiO$_2$ and H$_2$O/SiO$_2$ ratios on transformation of LEV

— Comparison with amorphous materials —

In order to better understand the LEV-CHA transformation, the influences of the

NaOH/SiO$_2$ and H$_2$O/SiO$_2$ ratios at a hydrothermal temperature of 125 °C were investigated. For comparison, zeolite synthesis was carried out via the conventional hydrothermal synthesis using Cab-O-Sil M-5 and NaAlO$_2$ as the starting Si and Al sources. Figure 5 shows the reactant composition diagram for these zeolite syntheses, which were carried out at 125 °C for 1.5 h using LEV-type zeolite and amorphous hydrogel (Cab-O-Sil M-5/NaAlO$_2$) as starting materials. This figure uses several symbols to stand for **the main zeolite phases** produced, and by-products are given below the main-product symbol.

When LEV-type zeolite was employed as the starting material, four types of zeolites, CHA, FAU, LTA, and SOD, were obtained. The less dense CHA- and LTA-type zeolites were obtained as pure phases. The FD of LTA-type zeolite is 14.2 T/1000 Å^3. On the other hand, only FAU- and SOD-type zeolites were obtained from amorphous **aluminosilicate hydrogels.** The fact that CHA- and LTA-type zeolites were not obtained from the starting gels under the present conditions strongly suggests that locally ordered aluminosilicate species generated by the decomposition/dissolution of the starting LEV-type zeolite contribute to crystallization of these zeolites. **Of course, we could not role out a strong influence of the silica source on the pathway of crystallization (transformation) and on the properties of the crystalline end**

products [35, 36].

LEV- and CHA-type zeolites have similar composite building units because these two zeolites both belong to chabazite group, whereas there was less similarity between the composite units of LEV- and LTA-type zeolites. These results strongly suggest that there is a large difference between the LEV-CHA and LEV-LTA interzeolite conversion behaviors. In contrast to the LEV-CHA transformation, the LEV-LTA transformation proceeded through the complete dissolution of the starting LEV-type zeolite. In other words, there was no product at crystallization times of 0.5−1 h, and the pure LTA-type zeolite was only obtained after 1.5 h of synthesis time. As can be seen in Figure 2 (d), the LTA-type zeolite morphology was cubic, and the crystal size was 2−5 μm. **As the starting LEV-type zeolite was decomposed under different alkalinity, it seems that there is a large difference in the structures of nanoparts generated by decomposition/dissolution of the starting zeolite in the LEV-CHA and LEV-LTA transformations. In the case of LEV-LTA transformation, there are probably some nanoprats, which are considerably decomposed and are not relevant for the transformation.**

Recently, Okubo et al. investigated the crystallization mechanism of low-silica faujasite X (LSX) by using a novel method with intermediate addition of alkaline metals

and the ion-exchange technique [37,38]. **When potassium caion was added to the starting gel containing sodium cation for synthesis of zeolite A, it was indicated that formation of a double six-membered ring (D6R) occurred by assembly of a four-membered ring (4R) in the liquid phase, resulting in selective formation of LSX in a precipitated hydrogel phase.**

On the basis of our result above, as well as the data obtained by Okubo et al., we can now speculate on the process of conversion of LEV-type zeolite into CHA- and LTA-type zeolites, as follows. At high alkalinity, $NaOH/H_2O$ = ($NaOH/SiO_2$ = 3.5)/(H_2O/SiO_2 = 40) = 0.088, it is expected that the starting LEV-type zeolite is decomposed into aluminosilicate species whose structure are different from the building units required for the crystallization of CHA-type zeolite. A simple 4R aluminosilicate is probably formed, resulting in the formation of LTA-type zeolite. Taking into account the fact that LTA-type zeolite could not form from the amorphous aluminosilicate hydrogels of Cab-O-Sil M-5 and $NaAlO_2$ **under the present hydrothermal synthesis condition, it is suggested that the use of LEV-type zeolite could effectively yield the 4R aluminosilicate species.** On the other hand, at lower alkalinity, $NaOH/H_2O$ = ($NaOH/SiO_2$ = 3)/(H_2O/SiO_2 = 80) = 0.038, locally ordered aluminosilicate species whose structures are similar to those of the precursor to CHA -type zeolite are formed,

resulting in the selective formation of CHA-type zeolite. **Of course, we have now no clear evidence for formation of nanoparts such as 4MRs or D6R. A further study concerning the chemical structures of nanoparts is now in progress.**

4. Conclusions

Hydrothermal conversion of LEV-type zeolite into CHA-type zeolite occurred in the absence of both OSDAs and seed crystals. Because the LEV-CHA transformation proceeds from a more dense zeolite (LEV) to a less dense one (CHA), the transformation is not thermodynamically favorable. **From the fact that transformation proceeded at lower alkalinity conditions, however, it was suggested that locally ordered aluminosilicate species (nanoparts) produced by decomposition/dissolution of the starting LEV-type zeolite contribute to the transformation process.** On the other hand, at higher alkalinity than that used for the CHA-type zeolite synthesis, LEV-LTA transformation occurred effectively and selectively. **It is possible to consider that simple four-membered ring aluminosilicate species, which are relevant for the transformation, are formed by the severe decomposition of LEV-type zeolite.**

Although the whole synthesis procedure of CHA-type zeolite was not OSDA-free, the findings of the present study indicate the possibility of transformation of dense

zeolite into less dense zeolite under mild conditions if there is similarity between the composite building units of the two zeolites. Therefore, the interzeolite conversion route has been again confirmed to be an alternative strategy for zeolite synthesis. **However, in order to establish the interzeolite conversion route as an alternative zeolite synthesis method, we have to understand the transformation process as well as chemical structures of locally aluminosilicate species generated from the starting zeolite.**

References

[1] J. Song, L. Dai, Y. Ji, F.-S. Xiao, Chem. Mater. 18 (2006) 2775.

[2] Z. Wu, J. Song, L. Ren, Y. Ji, J. Li, F.-S. Xiao, Chem. Mater. 20 (2008) 357.

[3] B. Xie, J. Song, L. Ren, Y. Ji, J. Li, F.-S. Xiao, Chem. Mater. 20 (2008) 4533.

[4] G. Majano, L. Delmotte, V. Valtchev, S. Mintova, Chem. Mater. 21 (2009) 4184.

[5] Y. Kamimura, W. Chaikitlisilp, K. Itabashi, A. Shimojima, T. Okubo, Chem. Asian J. 5 (2010) 2182.

[6] N. Ren, Z.-J. Yang, X.-C. Lv, J. Shi, Y.-H. Zhang, Y. Tang, Micropor. Mesopor. Mater. 131 (2010) 103.

[7] T. Yokoi, M. Yoshioka, H. Imai, T. Tatsumi, Angew. Chem. Int. Ed. 48 (2009) 9884.

[8] K. Iyoki, Y. Kamimura, K. Itabashi, A. Shimojima, T. Okubo, Chem. Lett. 39 (2010) 730.

[9] E.-P. Ng, D. Chateigner, T. Bein, V. Valtchev, S. Mintova, Science, 335 (2012) 70.

[10] M.E. Davis, R.F. Lobo, Chem. Mater. 4 (1992) 756.

[11] N.J. Henson, A.K. Cheetham, J.D. Gale, Chem. Mater. 6 (1994) 1647.

[12] P.M. Piccione, C. Laberty, S. Yang, M.A. Camblor, A. Navrotsky, M.E. Davis, J. Phys. Chem. B 104 (2000) 10001.

[13] B. Subotić, D. Škrtić, I. Šmit, L. Sekovanić, J. Cryst. Growth 50 (1980) 498.

[14] S.I. Zones, J. Chem. Soc. Faraday Trans. 87 (1991) 3709.

[15] Y. Kubota, H. Maekawa, S. Miyata, T. Tatsumi, Y. Sugi, Micropor. Mesopor. Mater. 101 (2007) 115.

[16] H. Jon, K. Nakahata, B. Lu, Y. Oumi, T. Sano, Micropor. Mesopor. Mater. 96 (2006) 72.

[17] H. Jon, S. Takahashi, H. Sasaki, Y. Oumi, T. Sano, Micropor. Mesopor. Mater. 113 (2008) 56.

[18] M. Itakura, T. Inoue, A. Takahashi, T. Fujitani, Y. Oumi, T. Sano, Chem. Lett. 37 (2008) 908.

[19] T. Inoue, M. Itakura, H. Jon, Y. Oumi, A. Takahashi, T. Fujitani, T. Sano, Micropor. Mesopor. Mater. 122 (2009) 149.

[20] H. Sasaki, H. Jon, M. Itakura, T. Inoue, T. Ikeda, Y. Oumi, T. Sano, J. Porous Mater. 16 (2009) 465.

[21] M. Itakura, Y. Oumi, M. Sadakane, T. Sano, Mater. Res. Bull. 45 (2010) 646.

[22] H. Jon, N. Ikawa, Y. Oumi, T. Sano, Chem. Mater. 20 (2008) 4135.

[23] K. Honda, A. Yashiki, M. Itakura, Y. Ide, M. Sadakane, T. Sano, Micropor.

Mesopor. Mater. 142 (2011) 161.

[24] A. Yashiki, K. Honda, A. Fujimoto, S. Shibata, Y. Ide, M. Sadakane, T. Sano, J. Cryst. Growth 325 (2011) 96.

[25] R.M. Barrer, L. Hinds, E.A. White, J. Chem. Soc. (1953) 1466.

[26] C.M. Zicovich-Wilson, F. Gándara, A. Monge, M.A. Camblor, J. Am. Chem. Soc. 132 (2010) 3461.

[27] P. Tian, X. Su, Y. Wang, Q. Xia, Y. Zhang, D. Fan, S. Meng, Z. Liu, Chem. Mater. 23 (2011) 1406.

[28] E. Loeffler, U. Lohse, Ch. Peuker, G. Oehlmann, L.M. Kustov, V.L. Zholobenko, V.B. Kazansky, Zeolites 10 (1990) 266.

[29] S.M. Alexander, D.M. Bibby, R.F. Howe, R.H. Meinhold, Zeolites 13 (1993) 441.

[30] D.E. Akporiaye, I.M. Dahl, H.B. Mostad, R. Wendelbo, J. Phys. Chem. 100 (1996) 4148

[31] H. Robson, K.P. Lillerud, "Verified Syntheses of Zeolitic Materials", second ed., Elsevier, Amsterdam, 2001, p. 123.

[32] H. Lechert, H. Kacirek, Zeolites 11 (1991) 720.

[33] A. Čižmek, B. Subotić, R. Aiello, F. Crea, A. Nastro, C. Tuoto, Microporous Mater. 4 (1995) 159.

[34] Z. Gabelica, N. Blom, E.G. Derouane, Appl. Catal. 5 (1983) 227.

[35] E.F. Freund, J. Cryst. Growth 34 (1976) 11.

[36] K.E. Hamilton, E.C. Coker, A. Sacco, A.G. Dixon, R.W. Thompson, Zeolites 13 (1993) 645.

[37] M. Iwama, Y. Suzuki, J. Plévert, K. Itabashi, M. Ogura, T. Okubo, Cryst. Growth Des. 10 (2010) 3471.

[38] M. Ogura, Y. Kawazu, H. Takahashi, T. Okubo, Chem. Mater. 15 (2003) 2661.

Table 1

Hydrothermal conversion of LEV and products obtained.

| Sample no. | Synthesis conditions[a] | | | | Product | | |
	Starting Si/Al ratio	NaOH/SiO$_2$	Temp. / °C	Time /h	Phase[b]	Bulk Si/Al ratio	Yield[c] / %
1	9	3.0	125	1.5	CHA	2.8	19
2	6	3.0	125	1.5	LEV		
3	12	3.0	125	1.5	CHA	2.6	21
4	22	3.0	125	1.5	No product		
5	9	3.0	170	1.5	CHA	3.1	20
6	9	3.0	200	1.5	ANA		
7	9	3.0	90	1.5	Am.		
8	9	3.0	90	12	CHA	4.9	20
9	9	3.0(LiOH)	125	1.5	Am. + Un.		
10	9	3.0(KOH)	125	1.5	Am.		
11	9	3.0(RbOH)	125	1.5	Am.		

[a] H$_2$O/SiO$_2$ = 80

[b] Am. = amorphous, Un. = unknown

[c]
$$\text{Yield (\%)} = \frac{\text{Product (g)}}{\text{Starting LEV zeolite (g)}} \times 100$$
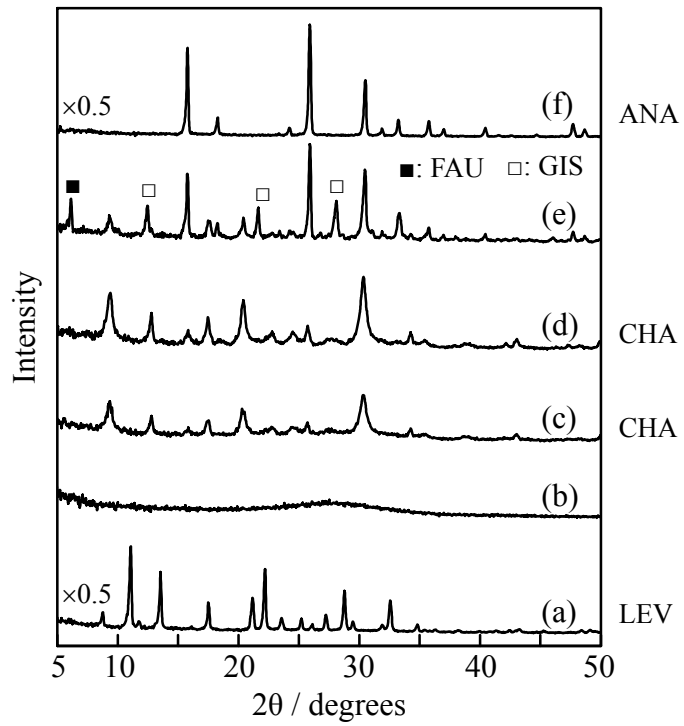
1

Figure captions

Fig. 1 Fig. 1 XRD patterns of products obtained from LEV (Si/Al = 9) after various crystallization times. (a) Starting LEV and (b–f) products after (b) 0.5 h, (c) 1 h, (d) 1.5 h, (e) 8 h, and (f) 24 h.
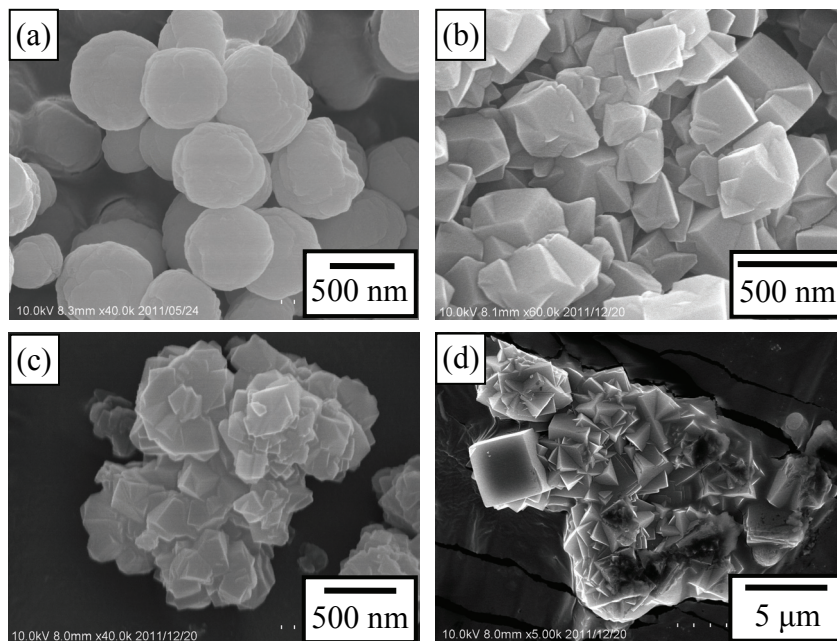
Fig. 2 SEM images of (a) starting LEV, (b) CHA (Sample no. 1), (c) CHA (Sample no. 8), and (d) the obtained LTA.
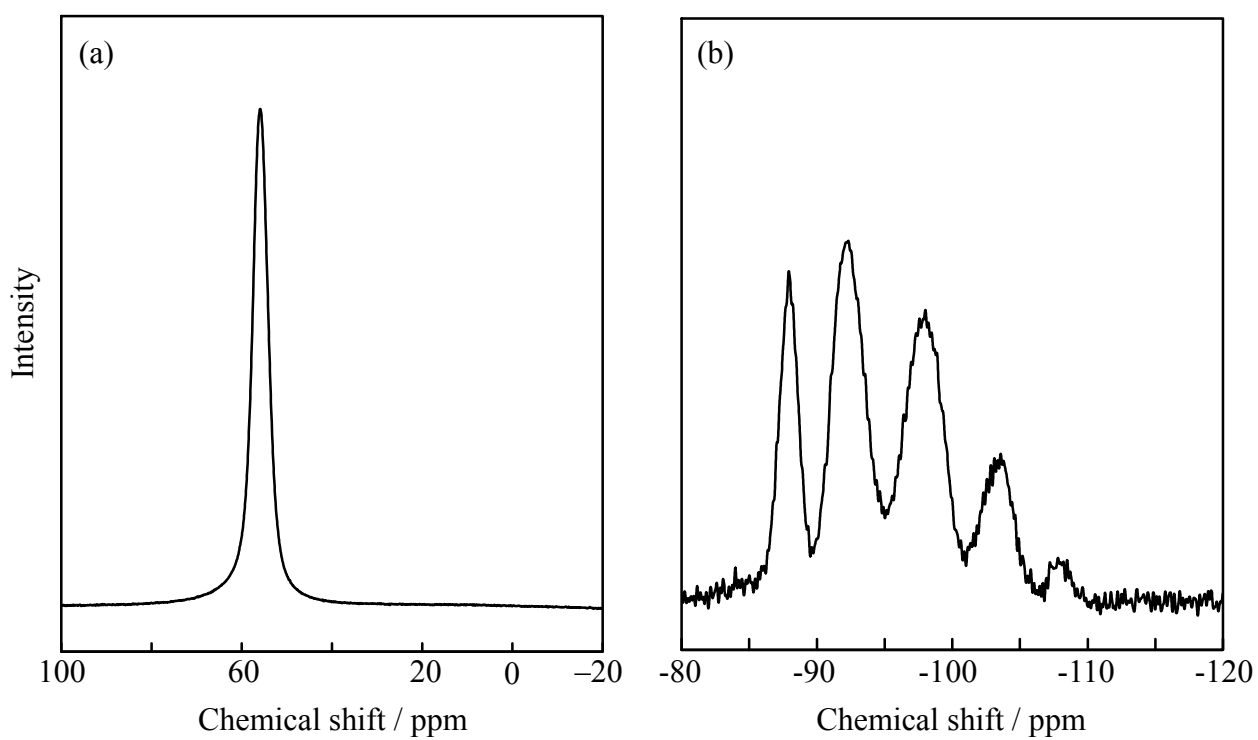
Fig. 3 (a) ^{27}Al and (b) ^{29}Si MAS NMR spectra of the obtained CHA (Sample no. 1).

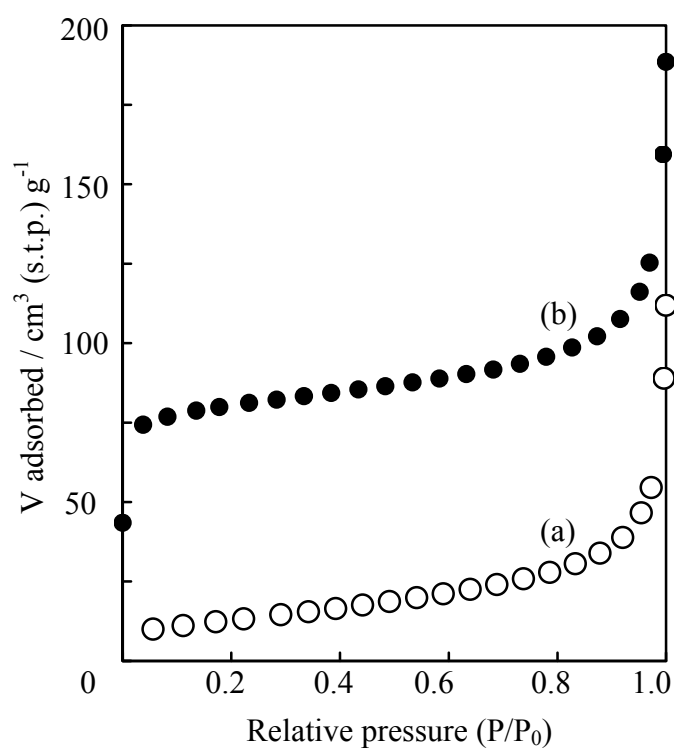Fig. 4 N_2 adsorption isotherms of the obtained (a) Na^+- and (b) Ca^{2+}- form CHA-type zeolites.

Fig. 5 Reactant composition diagram for zeolite syntheses at 125 °C for 1.5 h from (a) LEV (Si/Al = 9) and (b) Cab-O-Sil M-5/NaAlO$_2$.

Fig. 1 XRD patterns of products obtained from LEV (Si/Al = 9) after various crystallization times. (a) Starting LEV and (b–f) products after (b) 0.5 h, (c) 1 h, (d) 1.5 h, (e) 8 h, and (f) 24 h.

Fig. 2 SEM images of (a) starting LEV, (b) CHA (Sample no. 1), (c) CHA (Sample no. 8), and (d) the obtained LTA.

Fig. 3 (a) ^{27}Al and (b) ^{29}Si MAS NMR spectra of the obtained CHA (Sample no. 1).

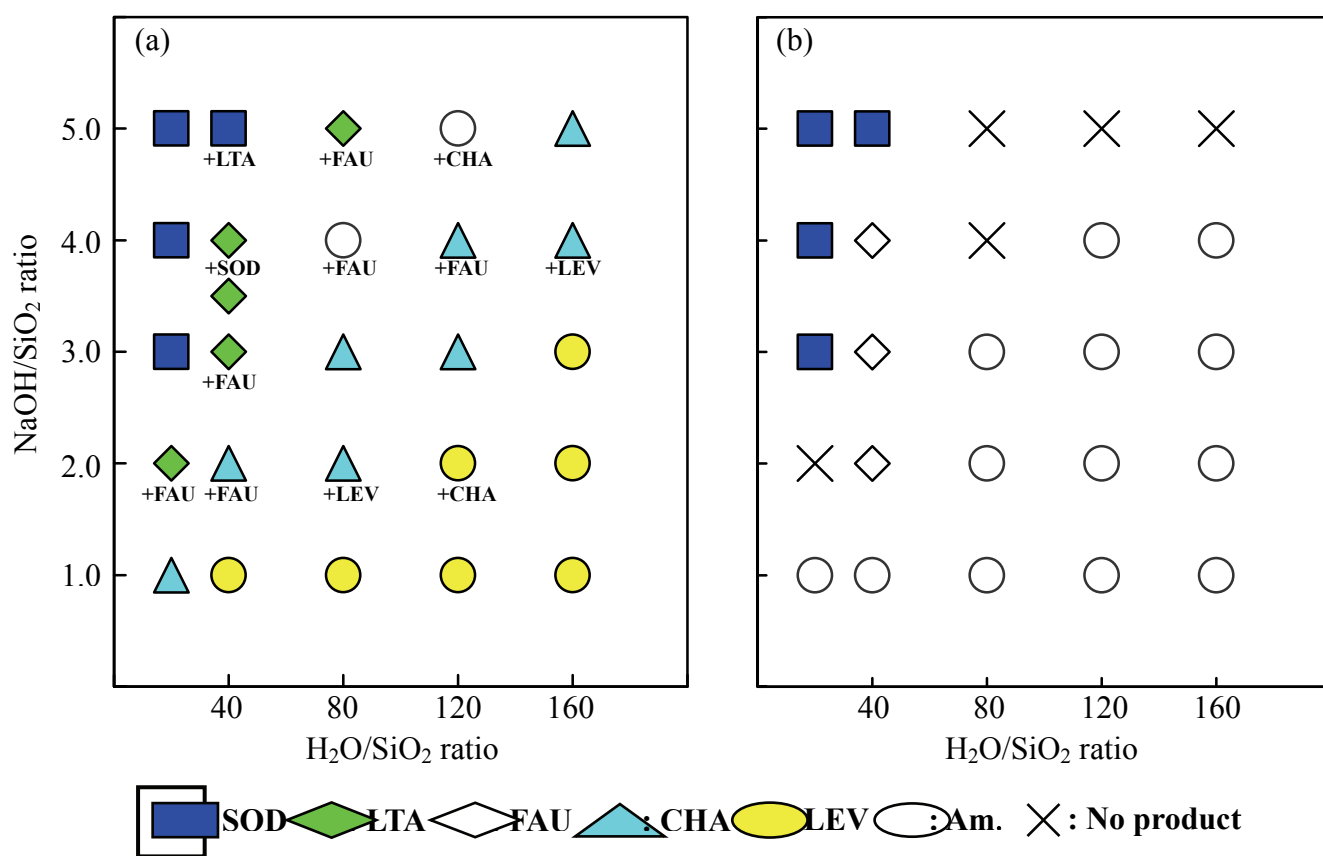Fig. 4 N_2 adsorption isotherms of the obtained (a) Na^+- and (b) Ca^{2+}- form CHA-type zeolites.

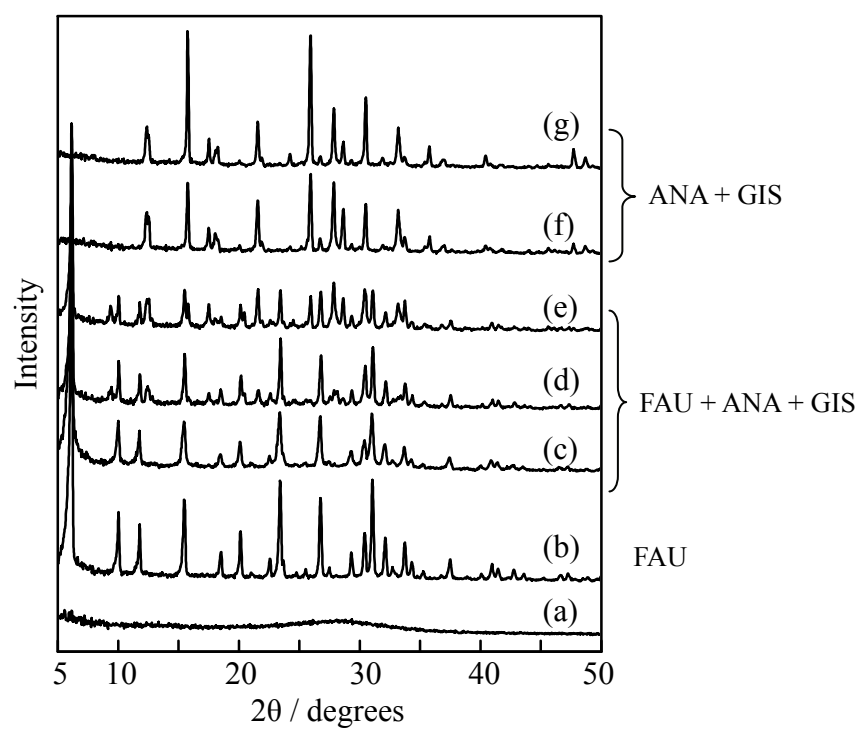Fig. 5 Reactant composition diagram for zeolite syntheses at 125 °C for 1.5 h from (a) LEV (Si/Al = 9) and (b) Cab-O-Sil M-5/NaAlO$_2$.

Figure 1S   XRD patterns of products obtained from Cab-O-Sil M-5 and NaAlO$_2$ (Si/Al = 9) after various crystallization times. (a) 1.5 h, (b) 3 h, (c) 12 h, (d) 1 d (e) 2 d, (f) 3 d, and (g) 7 d.